Domain Motion in Actin Observed by Fluorescence Resonance Energy Transfer†

Masao Miki*,‡ and Tsutomu Kouyama§

Department of Applied Chemistry and BioTechnology, Fukui University Fukui-shi 910, Japan, and The Institute of Physical and Chemical Research, Wako-shi 351, Japan

Received December 28, 1993; Revised Manuscript Received June 20, 1994®

ABSTRACT: Actin is composed of two well-separated globular domains which are further subdivided into two subdomains [Kabsch, W., Mannherz, H. G., Suck, D., Pai, E. F., & Holmes, K. C. (1990) *Nature 347*, 37–44]. Subdomains 1 and 2 constitute the small domain, and subdomains 3 and 4 comprise the large domain. In order to test a hinge bending domain motion in actin such as observed in many kinases, fluorescence resonance energy transfer between two probes attached to each of the two domains was measured by steady-state and time-resolved fluorometers. The adenine base is bound in a hydrophobic pocket between subdomains 3 and 4, and Tyr-69 is located at subdomain 2. In the present study, the adenine moiety was labeled with a fluorescence donor, εATP, and tyrosine-69 was labeled with the energy acceptor, dansyl chloride. Assuming the random orientation factor $\kappa^2 = {}^2/_3$, the distance between ε-adenine moiety and dansyl chloride attached to Tyr-69 in G-actin was determined to be 2.46 nm from steady-state fluorescence measurements. The addition of DNase I did not appreciably change the distance (less than 0.1 nm). The distance decreased to 2.27 nm during polymerization by the addition of phalloidin under physiological salt conditions. On the other hand, time-resolved fluorescence energy transfer measurements have been used to investigate a distribution of distances for a donor–acceptor pair. In G-actin, the mean distance between probes was 2.79 nm with a full width at half-maximum of 3.91 nm, indicating a large number of conformational substates in solution. Upon polymerization, the mean distance decreased to 2.22 nm, but the width of the distribution did not change. Further addition of tropomyosin and troponin in the presence and absence of Ca^{2+} did not significantly change the mean distance but decreased the width of the distribution appreciably. Upon addition of S1, the mean distance increased by 0.38 nm, and the width of the distribution decreased substantially.

Actin interacts with many other proteins and plays essential roles in eucaryotic cells. *In vitro,* actin exists in a monomeric form (G-actin) at low ionic strength and in a filamentous form (F-actin) under physiological conditions. Most of the actin functions are exhibited in its filamentous state. It is reported that actin changes its conformation during polymerization or interaction with other actin binding proteins [for a review, see Oosawa (1983)]. Recently, the atomic structure of actin has been revealed by X-ray crystallography (Kabsch et al., 1990). It consists of two well-separated domains. Subdomains 1 and 2 constitute the small domain, whereas subdomains 3 and 4 comprise the large domain. Based on the atomic structure, a normal mode analysis of G-actin describes the computed conformational changes in detail (Tirion, & Ben-Avraham, 1993). On the other hand, structures of several enzymes consist of two distinct domains separated by a wide cleft. In these enzymes, a hinge bending domain movement may play an important role in their catalytic activity (Haran et al., 1992; Holland et al., 1992; Sharff et al., 1992). By analogy to this, a domain movement in actin may play an important role in its physiological activity.

Fluorescence resonance energy transfer has been extensively used for studying the spatial relationships between residues on muscle proteins [for reviews, see Botts et al. (1984), dos Remedios et al. (1987), and Miki et al. (1992)]. This method is especially valuable for detecting a small conformational change, since the transfer efficiency is a function of the inverse of the sixth power of the distance between probes (Förster, 1948; Stryer & Haugland, 1967). In a previous report (Miki, 1991), two specific sites on actin, Tyr-69 and Cys-374, were labeled with fluorescence resonance energy donor and acceptor molecules, and the interprobe distance was measured under various conditions. No significant change in the distance in various states of actin (i.e., in complex with DNase I, in G-actin, in F-actin, etc.) was detected. The atomic model of actin locates Tyr-69 and Cys-374 in the same small domain but in different subdomains. It was concluded that the region involving Tyr-69 and Cys-374 is substantially rigid, and that a large deformation within the region does not occur.

According to the atomic structure of actin (Kabsch et al., 1990), the nucleotide is located at the cleft region with a calcium ion bound to the β-phosphate. The adenine base fits into a pocket formed by residues Lys-213, Glu-214, Thr-303, Met-305, Tyr-306, and Lys-336 which are located in the large domain, but there is no specific interaction between these amino acids and the adenine base. In the present paper, in order to test hinge bending domain movement in actin, the adenine base (on the large domain) is replaced with 1-N^6-ethenoadenosine (εATP)[1] as the resonance energy donor while Tyr-69 (on the small domain) is labeled with DNS-Cl as the energy acceptor. Then the distance between two probes is measured from fluorescence resonance energy transfer, and also changes in the distance are studied when G-actin forms

† This work was supported in part by a research grant from the Hokuriku Sangyo Kasseika Center.

* To whom correspondence should be addressed.
‡ Fukui University.
§ The Institute of Physical and Chemical Research.

® Abstract published in *Advance ACS Abstracts,* August 1, 1994.

[1] Abbreviations: S1, myosin subfragment 1; εATP, 1-N^6-ethenoadenosine 5′-triphosphate: dansyl chloride or DNS-Cl, 5-(dimethylamino)-naphthalene-1-sulfonyl chloride; DNS-actin, actin labeled at Tyr-69 with DNS-Cl; DNS-actin-εATP, actin labeled at Tyr-69 with DNS-Cl and at the nucleotide binding site with εATP; EGTA, ethylene glycol bis-(2-aminoethyl ether)-*N,N,N′,N′*-tetraacetic acid.

0006-2960/94/0433-10171$04.50/0

a complex with DNaseI, when it assembles into polymers (F-actin), and when F-actin interacts with myosin subfragment 1 or tropomyosin–troponin. In this report, we also measure fluorescence lifetimes of εATP or εADP bound to actin in the presence and absence of acceptor. In the absence of acceptor, the fluorescence decay of εATP or εADP can be described by a single decay constant, but in the presence of acceptor, the decay cannot be fitted with a single exponential decay curve, thus indicating a distribution of donor–acceptor distances. In the present report, fluorescence decay curves were analyzed by assuming a Gaussian distribution of donor–acceptor distances (Haas et al., 1975; Haran et al., 1992; James et al., 1992; Eis & Lakowicz, 1993). The results show that the mean distances are consistent with the values obtained from the steady-state measurements, and that the distribution of distances is very broad.

MATERIALS AND METHODS

Reagents. Phalloidin from *Amanita phalloides* was purchased from Boehringer Mannheim Biochemica. DNase I from bovine pancreas was from Worthington Biochemical Co. DNS-Cl was from Sigma Chemical Co. BCA protein assay reagent was from Pierce Chemicals. Tetranitromethane was synthesized according to the method of Liang (1941). εATP was synthesized according to the method of Secrist et al. (1972). All other chemicals were analytical grade.

Protein Preparations. Actin, S1, tropomyosin, and troponin were prepared as described in a previous report (Miki, 1990). Protein concentrations were determined from absorbance measurements, using absorption coefficients of $A_{290nm} = 0.63$ $(mg/mL)^{-1}$ cm^{-1} for G-actin (Lehrer & Kerwar, 1973) and $A_{280nm} = 0.75$ for S1 (Weeds & Pope, 1977), 0.33 for tropomyosin (Cummins & Perry, 1973), and 0.45 $(mg/mL)^{-1}$ cm^{-1} for troponin (Ishiwata & Fujime, 1972). Concentrations of DNase I and labeled actin were measured with the Pierce BCA protein assay reagent, using unlabeled actin as the standard. Relative molecular masses of 42 000 for actin, 115 000 for S1, 66 000 for tropomyosin, 69 000 for troponin, and 31 000 for DNase I were used.

Labeling of Actin at Tyr-69 with DNS-Cl. Tyr-69 in actin was nitrated with tetranitromethane, and then DNS-Cl was introduced in to this residue according to the method of Chantler and Gratzer (1975) with a slight modification (Miki et al., 1987). The labeling ratio of DNS-Cl to actin was determined to be 1.0, using an absorption coefficient for dansyl of 4600 M^{-1} cm^{-1} at 335 nm (Kenner & Neurath, 1971). Labeled actin was lyophilized in the presence of 0.1 M sucrose and kept at −20 °C.

Double Labeling of Tyr-69 and of the Nucleotide Binding Site. Actin labeled at Tyr-69 with DNS-Cl (DNS-actin) was further modified with εATP. DNS-actin (about 1.5 mg/mL) in 1 mM Tris-HCl (pH 8.0), 0.1 mM ATP, and 0.1 mM $CaCl_2$ was mixed with a $^1/_{10}$ volume of Dowex-I on ice. After 5 min, Dowex-I was removed by passing through a filter syringe, and 1 mM εATP was added immediately. The sample was dialyzed exhaustively against 1 mM Tris-HCl (pH 8.0), 0.1 mM $CaCl_2$, and 0.2 mM εATP. Then the solution was clarified by ultracentrifugation at 100000*g* for 2 h. Just prior to fluorescence measurements of G-actin, free εATP was removed by the treatment with Dowex-I as described above. For preparation of DNS-F-actin-εADP, DNS-G-actin-εATP (2 mg/mL) was treated with Dowex-I and was immediately polymerized in 4 mM $MgCl_2$, 20 mM Tris-HCl (pH 7.6), 30 mM KCl, and 2 mM NaN_3 (buffer F) in the presence of a 2-fold molar excess of phalloidin (Miki et al., 1987).

Spectroscopic Measurements. Absorption was measured with a Hitachi U2000 spectrophotometer. Steady-state fluorescence was measured with a Hitachi 850 fluorometer. Sample cells were placed in a thermostated cell holder. For fluorescence intensity measurements, the exciting light was polarized at 35° in order to compensate for the effect of rotational motion of chromophores. Fluorescence lifetime and anisotropy decay measurements were carried out with a single photon counting apparatus as described previously (Kouyama et al., 1989). For each experiment, we measured the following three experimental curves: the response function $g(t)$ obtained with a dilute Ludox (Du Pont) suspension in place of sample, the parallel $i_v(t)$ and perpendicular $i_h(t)$ components of the polarized fluorescence. Fluorescence decay and anisotropy decay curves were analyzed by the moments method (Small & Isenberg, 1976) and an iterative least-square method. Excitation wavelength for εATP was at about 320 nm, using a monochromator and a UV 340 broad band pass filter, and emission from 400 to 450 nm was collected by use of a broad band cut filter (Asahi Bunko Co.) and an SC39 cutoff filter (Fuji film). In order to eliminate the contribution of the acceptor (DNS-Cl) fluorescence, we prepared the same concentration of DNS-actin without εATP/ADP as a reference sample. The transient fluorescence emission of the reference sample observed under the same experimental conditions was subtracted from the fluorescence of the studied solution. The fluorescence intensity of the reference solution was usually less than 6% of the intensity of the sample solution.

Fluorescence Resonance Energy Transfer. The efficiency, E, of resonance energy transfer between probes was determined by measuring the fluorescence intensity of the donor both in the presence (F_{DA}) and absence (F_{D0}) of the acceptor as given by

$$E = 1 - F_{DA}/F_{D0} \tag{1}$$

According to Förster's theory [for reviews, see Fairclough and Cantor (1978), Stryer (1978), and Lakowicz (1980)], the efficiency is related to the distance (R) between probes and Förster's critical distance (R_0) at which the transfer efficiency is equal to 50% by

$$E = R_0^6/(R_0^6 + R^6) \tag{2}$$

R_0 can be obtained (in nm) by

$$R_0^6 = (8.79 \times 10^{-11}) n^{-4} \kappa^2 Q_{D0} J \tag{3}$$

where n is the refractive index of the medium taken to be 1.4, κ^2 is the orientation factor, Q_{D0} is the quantum yield of the donor in the absence of the acceptor, and J is the spectral overlap integral (in M^{-1} cm^{-1} nm^4) between the donor emission $F_D(\lambda)$ and acceptor absorption $\epsilon_A(\lambda)$ spectra defined by

$$J = \int F_D(\lambda)\epsilon_A(\lambda)\lambda^4 \, d\lambda / \int F_D(\lambda) \, d\lambda \tag{4}$$

The quantum yield of free εATP in 10 mM phosphate buffer at pH 7.0 was found to be 0.45, taking the quantum yield of quinine sulfate of 0.53 as the standard (Kouyama et al., 1985). Quantum yields of bound εATP/ADP in actin were determined by assuming that the quantum yield is proportional to the fluorescence lifetime. The fluorescence lifetime of free εATP was 25.6 ns at 23 °C in 10 mM phosphate buffer at pH 7.0. κ^2 was taken as $^2/_3$ for calculation of distances, and the maximum and minimum values of κ^2 were estimated according to the method of Dale et al. (1979).

$$\kappa^2_{max} = (2/3)(1 + d_A + d_D + 3d_A d_D) \quad (5)$$

$$\kappa^2_{min} = (2/3)[1 - (d_A + d_D)/2] \quad (6)$$

where $d_A = (r_{A0}/r_{Af})^{1/2}$, $d_D = (r_{D0}/r_{Df})^{1/2}$, r_{A0} and r_{D0} are the limiting anisotropies of the donor and acceptor, respectively, and r_{Af} and r_{Df} are the fundamental anisotropies of the donor and acceptor, respectively. Using these values for the orientation factor instead of $^2/_3$, the maximum (R_{max}) and minimum (R_{min}) distances between probes are calculated.

Time-resolved fluorescence decay curves in the presence of acceptor were analyzed by assuming a Gaussian distribution of donor–acceptor distances (Eis & Lakowicz, 1993; Haran et al., 1992). Using the distance probability distribution $P(r)$, the fluorescence decay curve can be written as

$$f(t) = \int dr\, P(r) \exp[-[1 + (R_0/r)^6]t/\tau_0] \quad (7)$$

Here $P(r)$ can be written as

$$P(r) = \alpha \exp[-(r - R_{av})^2/2\sigma^2] \quad (8)$$

where α is the normalizing factor, R_{av} is the average distance (most probable distance), and σ is the standard deviation of the untruncated Gaussian function. The half-width of the distribution (FWHM, full width at half-maximum probability) is 2.355σ in the Gaussian model. The fluorescence decay function $f(t)$ was then convoluted with the measured response function of the apparatus to get the calculated intensity decay $i_c(t)$, which was compared with the measured decay data $i_e(t)$. The goodness of the fit was judged by the reduced χ^2, which is defined as $(1/N)\sum_{i=1}^{N}(I_{c,i} - I_{e,i})^2/I_{e,i}$, where $I_{c,i}$ and $I_{e,i}$ are calculated and experimental intensities in the ith channel, respectively, and N is the number of channels. The χ^2 value should be close to 1.0 for a good fit.

RESULTS

Spectral Relation of Donor and Acceptor. Figure 1 shows the emission spectrum of ϵATP-G-actin and the absorption spectrum of DNS-Cl bound to actin. The overlap integral was calculated according to eq 4. J was calculated to be 1.278×10^{13} M^{-1} cm^{-1} nm^4. By taking $n = 1.4$, $\kappa^2 = ^2/_3$, and the quantum yields of 0.60, 0.60, 0.56, 0.53, 0.56, 0.55 for bound ϵATP/ADP in G-actin, G-actin/DNase I complex, F-actin, F-actin/S1 complex, F-actin/Tm/Tn/+Ca, and F-actin/Tm/Tn/–Ca, Förster's critical distances R_0 were calculated to be 2.21, 2.21, 2.19, 2.17, 2.19, and 2.18 nm, respectively.

Steady-State Fluorescence Measurements of Transfer Efficiency. In order to obtain the transfer efficiency between ϵATP and DNS-Cl in G-actin, the fluorescence intensity of DNS-G-actin-ϵATP was compared with that of G-actin-ϵATP. Just before fluorescence measurements, free ϵATP was removed from the sample solution by Dowex-I treatment as indicated under Materials and Methods. The emission of G-actin-ϵATP and DNS-G-actin-ϵATP excited at 330 nm was measured at 15 °C. Actin concentration was 0.2 mg/mL. Although the protein concentrations in samples were adjusted to be the same, the concentrations of fluorophore were not exactly the same because the preparation procedure was not exactly the same between G-actin-ϵATP and DNS-G-actin-ϵATP. The ratio of these fluorescence intensities is proportional to $(F_{DA} \times C_i)/(F_{D0} \times C_{i0})$, where C_i and C_{i0} are the concentrations of ϵATP in DNS-G-actin-ϵATP and G-actin-ϵATP, and F_{DA} and F_{D0} are the fluorescence intensities

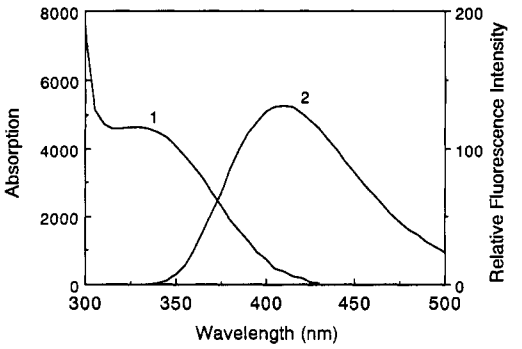

FIGURE 1: Spectral overlap of the absorption spectrum of DNS-Cl attached to Tyr-69 on actin (1) and the fluorescence spectrum of ϵATP bound to G-actin excited at 330 nm (2). Spectra were measured in 2 mM Tris-HCl (pH 8.0) and 0.1 mM $CaCl_2$ at 15 °C.

of DNS-G-actin-ϵATP (in the presence of acceptor) and G-actin-ϵATP (in the absence of acceptor), respectively. Since the fluorescence intensity depends on the concentration of the fluorophore in the sample solution, the reference fluorescence intensity must be measured in order to normalize it by the fluorophore concentration. Moreover, the existence of the acceptor molecule may decrease the fluorescence intensity not only through resonance energy transfer but also through inner filter effects. From the absorptions at the excitation (A_{ex}) and emission (A_{em}) wavelengths, the decrease of the fluorescence intensity due to inner filter effects can be estimated by use of the following equation, when a 1×1-cm^2 cuvette is illuminated centrally and observed at a right angle (Lakowicz, 1983; Miki, 1990, 1991).

$$F_{obs} = F_{corr} \times 10^{-(A_{ex}+A_{em})/2} \quad (9)$$

where F_{obs} and F_{corr} are the observed and correct fluorescence intensities, respectively. In the present case (DNS-ϵATP-actin), inner filter effects decrease the fluorescence intensity by about 2.5% when excited at 330 nm and measured at 410 nm. These factors should be taken into account when the transfer efficiency is calculated. For this purpose, 2 mM ATP was added to the sample solution after the fluorescence measurements. Under these conditions, ϵATP is released from G-actin and the donor and the acceptor are separated, and then resonance energy transfer no longer occurs. One can expect that the fluorescence intensity is now directly proportional to the concentration of ϵATP in the sample solution (C_i/C_{i0}) with a small modification by the inner filter effects, since ϵATP is now free in the solution and both F_{DA} and F_{D0} are changed to F_{Dfree}, where F_{Dfree} is the fluorescence intensity of free ϵATP in the solution. By the addition of ATP, the contribution of the inner filter effects does not change, since the absorptions at 330 and 410 nm remain unchanged. Taking this correction factor into account, the inner filter effects are canceled out, and the ratio of the fluorescence intensity of DNS-G-actin-ϵATP to that of G-actin-ϵATP (F_{DA}/F_{D0}) can be determined, and finally the transfer efficiency is obtained as 0.343 ± 0.03. This value corresponds to the distance of 2.46 ± 0.06 nm.

The effect of DNase I on the transfer efficiency was measured. The fluorescence intensities of DNS-G-actin-ϵATP and G-actin-ϵATP were compared in the presence of 0.2 mg/mL DNase I as described above. The transfer efficiency was determined to be 0.330 ± 0.03, which corresponds to the distance of 2.48 ± 0.07 nm.

The effect of polymerization on the transfer efficiency was measured. After removing free ϵATP by treatment with

Table 1: Distances between ϵATP (the Adenine Binding Site) and Dansyl Chloride (Tyr-69) in Actin[a]

sample	transfer efficiency	distance (nm) R_{min}	$R(2/3)$	R_{max}	limiting anisotropy r_0
G-actin	0.343	1.82	2.46	3.19	0.242
G-actin/DNase I	0.330	1.65	2.48	3.28	0.290
F-actin	0.444	1.68	2.27	2.94	0.207
F-actin/Tm/Tn/+Ca	0.433	1.69	2.29	2.97	0.193
F-actin/Tm/Tn/−Ca	0.437	1.68	2.27	2.94	0.190
F-actin/S1	0.381	1.69	2.35	3.07	0.231

[a] The experimental errors in the transfer efficiency were ±0.04, which corresponds to the error less than 0.1 nm in calculation of $R(2/3)$.

Dowex I, DNS-G-actin-ϵATP and G-actin-ϵATP were polymerized in buffer F by the addition of a 2-fold molar excess of phalloidin. A part of these G-actin samples was used for determination of the ratio of bound ϵATP of DNS-G-actin-ϵATP to that of G-actin-ϵATP. This ratio was used as the correction factor for fluorophore concentration (including the inner filter effects) on determination of the transfer efficiency as above mentioned. The emission spectra of DNS-F-actin-ϵADP and F-actin-ϵADP were measured in buffer F at 410 nm and 15 °C. The concentration of actin was 0.1 mg/mL. The emission peak of G-actin-ϵATP did not change during polymerization, but the fluorescence intensity decreased slightly (7%). This decrease in the fluorescence intensity can be attributed to the decrease of the quantum efficiency, since the fluorescence lifetime of F-actin-ϵADP is 6% smaller than that of G-actin-ϵATP (Table 2). By comparing the fluorescence intensities of F-actin-ϵADP and DNS-F-actin-ϵADP, the transfer efficiency was determined to be 0.444 ± 0.04, which corresponds to the distance of 2.27 ± 0.06 nm.

The effects of S1 binding on the transfer efficiency was measured. Highly concentrated S1 (10.4 mg/mL) was added into the above samples (the final concentrations of actin and S1 were 0.1 and 0.26 mg/mL, respectively). The addition of S1 decreased the fluorescence intensity of F-actin-ϵADP by 9%. On the other hand, the fluorescence lifetime of F-actin-ϵ-ADP decreased by 6% by the addition of S1 (Table 2). The difference (3%) could be attributed to the increase of the scattering light in the presence of S1. In order to cancel out these effects, the emission spectrum of the F-actin-ϵADP/S1 complex was taken as the reference which is compared with that of the DNS-F-actin-ϵADP/S1 complex. Thus the transfer efficiency in the presence of S1 was calculated to be 0.382 ± 0.04, which corresponds to the distance of 2.35 ± 0.07 nm.

The effects of tropomyosin–troponin in the presence and absence of Ca^{2+} on the transfer efficiency was measured at 15 °C. The concentrations of actin, tropomyosin and troponin were 0.1, 0.025, and 0.025 mg/mL, respectively. The fluorescence intensities of F-actin-ϵADP/tropomyosin/troponin were compared with those of DNS-F-actin-ϵADP/tropomyosin/troponin in buffer F and 0.1 mM $CaCl_2$ (in the presence of Ca^{2+}) or 1 mM EGTA (in the absence of Ca^{2+}), and the transfer efficiencies were determined to be 0.433 ± 0.04 in the presence of Ca^{2+} and 0.437 ± 0.04 in the absence of Ca^{2+}, which correspond to the distances of 2.29 ± 0.06 and 2.27 ± 0.07 nm, respectively. Transfer efficiencies and distances of each samples are summarized in Table 1. The maximum and minimum distances are also calculated by use of eqs 5 and 6 and summarized in Table 1.

Time-Resolved Fluorescence Measurements of Transfer Efficiency. Fluorescence lifetimes of ϵATP/ADP bound to actin were measured under the same solvent conditions as steady-state fluorescence measurements by a single photon

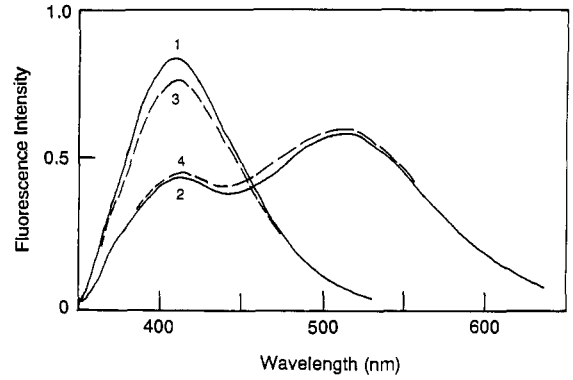

FIGURE 2: Fluorescence spectra of F-actin-ϵADP (1 and 3) and DNS-F-actin-ϵADP (2 and 4). Excitation wavelength was 330 nm. Protein concentrations were 0.1 mg/mL actin (1 and 2, solid lines) and 0.26 mg/mL S1 (3 and 4, broken lines) in 30 mM KCl, 4 mM $MgCl_2$, 20 mM Tris-HCl (pH 7.6), and 2 mM NaN_3 at 15 °C.

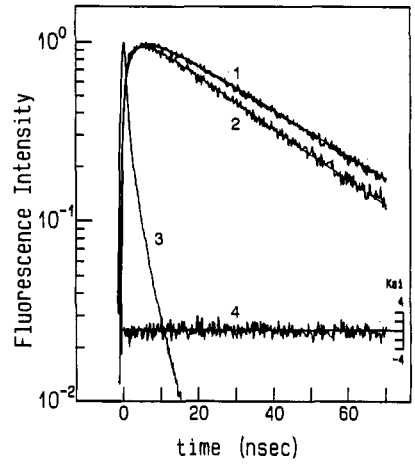

FIGURE 3: Fluorescence decay curves of G-actin-ϵATP (1) and DNS-G-actin-ϵATP (2), and the response function of the apparatus (3). Notched lines are experimental curves, and smooth lines are calculated fits. (1) Decay was fitted to a single-exponential function (τ = 34.2 ns). (2) Fit is from a detailed energy transfer analysis. The curve at the bottom (4) shows the difference function, D for the DNS-G-actin-ϵATP data. D is defined as $(I_{c,i} - I_{e,i})/(I_{e,i})^{1/2}$, where $I_{c,i}$ and $I_{e,i}$ are calculated and experimental fluorescence intensities, respectively, in the ith channel.

counting method. In the presence of a sufficient amount of Ca^{2+}, ATP binds tightly to G-actin with the affinity of 10^{10} M^{-1} (Engel et al., 1977). The affinity of ϵATP is one-fifth that of ATP (Neidl & Engel, 1979). Under our experimental conditions, G-actin-ϵATP samples were stable within the period of measurement as previously reported (Miki & Wahl, 1984). The fluorescence decay curve of ϵATP/ADP bound to actin in the absence of acceptor can be analyzed with a single exponential lifetime (Figure 3 and Table 2). On the other hand, the fluorescence decay curve of ϵATP/ADP bound to actin in the presence of acceptor (DNS-Cl) cannot be fitted satisfactorily with a single lifetime, since the χ^2 values (goodness of the fit) were very large (5.2 for G-actin, 6.6 for G-actin/DNase I, 7.5 for F-actin). The results suggest a distribution of donor–acceptor distances (Haas et al., 1975). Therefore, the fluorescence decay curves in the presence of acceptor were analyzed by use of eq 7, assuming a Gaussian distribution of the donor–acceptor distances as eq 8. Fluorescence decay and distance distribution parameters are summarized in Table 2. Typical fluorescence decay curves of G-actin-ϵATP and DNS-G-actin-ϵATP in 1 mM Tris-HCl (pH 8.0) and 0.1 mM $CaCl_2$ at 15 °C are shown in Figure 3. The χ^2 value and weighted deviation function showed that the curve fitting is satisfactory. The calculated interprobe

Table 2: Distance Distribution Parameters[a]

sample	τ_0 (ns)	mean distance (nm)	FWHM (nm)	χ^2
G-actin	34.20	2.79 (2.4)	3.91 (3.2)	1.21 (1.19)
G-actin/DNase I	34.49	2.86 (2.4)	3.91 (3.0)	1.65 (1.93)
F-actin	32.11	2.22 (1.9)	3.99 (3.0)	1.08 (1.08)
F-actin/Tm/Tn/+Ca	32.11	2.37 (2.1)	3.33 (2.4)	1.78 (1.73)
F-actin/Tm/Tn/−Ca	31.34	2.37 (2.0)	3.00 (2.3)	1.31 (1.26)
F-actin/S1	30.27	2.60 (2.2)	3.00 (2.0)	1.25 (1.25)

[a] τ_0 is the fluorescence lifetime of εATP/ADP bound to actin in the absence of acceptor. The SD error levels in the mean distance and FWHM are ±0.1 nm and ±0.2 nm, respectively. Values in parentheses are calculated assuming that the labeling ratio of acceptor is 0.8 in order to estimate the effect of labeling heterogeneity.

distance distributions are plotted in Figure 4. The mean interprobe distance in G-actin, 2.79 ± 0.1 nm, is slightly longer than the value of 2.46 nm determined from steady-state fluorescence measurements. The distribution is very broad, with a FWHM = 3.91 ± 0.2 nm, suggesting considerable flexibility in the structure of actin. Similar sets of measurements were carried out for G-actin/DNase I, F-actin, F-actin/S1, and F-actin/Tm/Tn in the presence and absence of Ca^{2+} (Table 2). Polymerization caused a decrease of the mean interprobe distance by 0.5 nm but no appreciable change in FWHM. The addition of S1 to F-actin increased the mean interprobe distance by 0.3 nm and also narrowed the width of the distance distribution significantly. The addition of tropomyosin and troponin did not change the mean interprobe distance appreciably but decreased FWHM significantly both in the presence and absence of Ca^{2+}.

Anisotropy decay measurements of εATP bound to G-actin gave a single rotational correlation time of 34.1 ns at 15 °C, suggesting that εATP binds tightly to G-actin. The zero-time value of the anisotropy decay (the limiting anisotropy r_0) was 0.242. These values are in good accordance with the values reported previously (Mihashi & Wahl, 1975). The rotational correlation time and the limiting anisotropy of εATP bound to G-actin increased to 89.1 ns at 15 °C and to 0.290, respectively, by the addition of DNase I, suggesting that εATP binds tightly to the actin-DNase I complex. Anisotropy decay measurements of εADP bound to F-actin gave the rotational correlation time longer than 1 μs as previously reported (Mihashi & Wahl, 1975). The addition of tropomyosin and troponin or S1 did not change the anisotropy decay. The r_0 values are summarized in Table 1. These anisotropy decay measurements indicate that the rotational freedom of εATP/ADP at the nucleotide binding site of actin is strongly depressed in the nanosecond time scale except for a subnanosecond time scale hindered rotational motion (Kinosita et al., 1977) or a much slower motion in a millisecond time scale.

DISCUSSION

Domain Motion. The polymerization of G-actin induces a large decrease of 0.5 nm in the average distance between the probes attached to the two domains but not a substantial change in the distribution of distances. In order to avoid effects of the neighboring acceptors in the F-actin filament on the fluorescence resonance energy transfer, we used a donor–acceptor pair which has a short critical distance R_0 of 2.2 nm. According to an F-actin model based on the crystal structure by Holmes et al. (1990), the intramonomer distance of N^6 of adenine and C_α of Tyr-69 is 2.15 nm, while the nearest and the second nearest neighboring intermonomer distances are 3.99 and 4.00 nm, respectively. Because the transfer efficiency

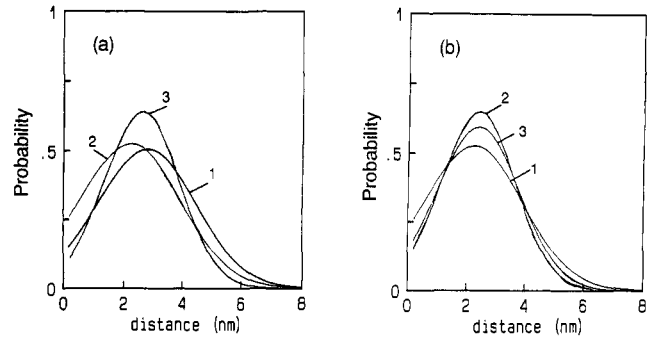

FIGURE 4: (a and b) Interprobe equilibrium distance distribution function of G-actin (a-1), F-actin (a-2 and b-1), F-actin/S1 (a-3), F-actin/Tm/Tn/−Ca (b-2), and F-actin/Tm/Tn/+Ca (b-3).

depends on the sixth power of the distance between the donor and acceptor molecules, the effect of the neighboring acceptor by a filament formation on the energy transfer efficiency is negligibly small (only 3.6%). In the present study, the transfer efficiency between εATP and DNS-Cl on actin changed 30% during polymerization. It was therefore concluded that the change of the transfer efficiency by polymerization is mainly due to a change of the distance between probes in the actin protomer in an F-actin filament.

Tirion and ben-Avraham (1993) analyzed the vibrational modes of G-actin to yield a complete description of the motion in vacua in the 0.1–17.0-ps time scale. The normal mode analysis demonstrated domain and subdomain motions of G-actin: a propeller-like twisting of the large and small domains and a scissor-type opening and closing of the cleft between two domains. It also showed very flexible regions in subdomains 2 (residues 34–55) and 4 (residues 230–250), and fixed regions or hinges. Fluorescence resonance energy transfer measurements showed that the polymerization of G-actin induces a significant decrease in the distance between Tyr-69 and the adenine binding site but no substantial decrease in the distance between Tyr-69 and Cys-374 (Miki, 1991). The results suggest that a domain motion of actin occurs during polymerization without a large deformation of the small domain (at least the region including Tyr-69 and Cys-374). Recently, Lorenz et al. (1993) have carried out a refinement of the F-actin model against X-ray diffraction data on oriented F-actin gels, by permitting structural changes of smaller parts of the actin monomer as well as domain motions. They reported that the cleft between subdomains 2 and 4 becomes smaller upon polymerization in accordance with the present results.

Effects of DNase I, S1, or Tropomyosin–Troponin Binding. Anisotropy decay measurements showed that DNase I forms a complex with DNS-G-actin. However, DNase I binding to actin did not change appreciably the average interprobe distance or the width of the distribution. This is rather surprising since DNase I inhibits the exchange of bound nucleotide (εATP) in actin (Mannherz et al., 1980) and also protects DNS-G-actin from denaturation (Miki, 1991). On the other hand, the limiting anisotropy of εATP bound to G-actin is substantially larger in the presence of DNase I than that in the absence of DNase I. This suggests that the pocket for the adenine base in G-actin became narrow by the addition of DNase I and consequently that the wobbling motion of the adenine base in the nucleotide binding site was suppressed, resulting in reduction of the nucleotide exchange rate. The addition of S1 increases the average distance by 0.3 nm and also decreases the width of the distance distribution substantially. An opening of the domains may increase an exchange rate of the bound nucleotide in F-actin.

The interaction of actin with myosin is regulated by tropomyosin and troponin in response to a change of Ca^{2+} concentration. The regulation mechanism is still not clear. On the other hand, there are a number of examples indicating that a hinge bending domain motion is an essential component of catalytic activity in enzymes which are composed of two globular domains separated by a wide cleft (Bennett & Huber, 1984; Ringe & Petsko, 1985; Holland et al., 1992; Sharff et al., 1992). In analogy to this, a movement of two domains of actin may be essential to the regulation mechanism; i.e., on-state and off-state of the thin filament. In previous papers (Miki, 1990; Miki & Iio, 1992), we reported that the distance between Lys-61 on actin and Cys-133 on TnI in reconstituted filaments changed by 0.5–0.6 nm in response to a change of Ca^{2+} concentration. We suggested that this change in the distance could be attributed to a movement of TnI on the thin filament or else a distortion of actin protomers (including a relative movement of two domains) in the thin filament. Lys-61 is located on the same subdomain as Tyr-69. The present results showed no substantial movement of domains of actin protomers on the reconstituted thin filament in response to a change of Ca^{2+} concentration. Therefore, the change in the distance between Lys-61 on actin and Cys-133 on TnI in the reconstituted thin filament can be attributed mainly to a movement of TnI on the thin filament. This movement of TnI is a triggering step for the regulation mechanism of skeletal muscle thin filaments by troponin–tropomyosin. However, we do not rule out any other conformational change of actin protomers on thin filaments induced by tropomyosin–troponin [for a review, see Oosawa (1983)]. The addition of tropomyosin–troponin appreciably narrowed the width of the distribution but did not change the interprobe distance (Figure 4). The width of the distribution did not change significantly in response to a change in Ca^{2+} concentration.

Distance Distribution. Time-resolved fluorescence measurements indicate the wide distribution of distance between the two labeled sites (the adenine portion and Tyr-69). The standard deviation of the distribution is 1.66 nm in the case of G-actin, corresponding to a full width at half-maximum height of 3.91 nm. This value was obtained on the assumption of the complete labeling of Tyr-69 with DNS-Cl. A smaller value is calculated if a fraction of the actin molecule is not labeled with DNS-Cl. The labeling ratio of the acceptor was determined from the absorbance measurements, assuming that the extinction coefficient of DNS attached to actin is the same as ethyl α-*N*-acetyl-3-(1′-dimethylaminonaphthalene-5′-sulfonamido)tyrosinate (Kenner & Neurath, 1971). Due to a difference of the extinction coefficient and also to some extent the heterogeneity of the labeling sites, the real ratio of acceptor to donor may be slightly different from 1.0. In order to estimate the effect of the labeling ratio of the acceptor on the mean distance and FWHM, we examined an extreme case in which the labeling ratio was assumed to be 0.8. Table 2 shows the calculated mean distances and FWHM. Both the values of mean distances and FWHM decreased considerably, but these calculation still gave very broad distributions and did not dramatically affect the differences observed between G-actin, G-actin/DNase I, F-actin, F-actin/Tm/Tn/+Ca, F-actin/Tm/Tn/–Ca, and F-actin/S1. A more extreme case may be excluded because the fitting of fluorescence decay curves became worse when a further lower labeling ratio was assumed.

The rms deviation from the crystallographic coordinates derived from normal mode analysis is at least one order magnitude smaller than that of the present distribution of distances. It should be noted here that the distance distribution derived from the present analysis is an apparent one (James et al., 1992). Real distance heterogeneity, orientational disorder, and the length of the linker arms of probes all may contribute to the apparent distribution of distances. Here the potential contribution of the orientational factor to the width of a distance distribution was estimated. In the present calculation of distances, a random orientation factor $k^2 = {}^2/_3$ was used. The anisotropy decay measurements showed that the donor molecule is rigidly confined in actin, indicating that the random orientation factor is not the case. However the limiting anisotropy r_0 of ϵATP/ϵADP bound to actin (Table 1) is considerably lower than its fundamental anisotropy of 0.33 (P = 0.42 at –50 °C; Secrist et al., 1972), suggesting a limited rapid rotation of the adenine moiety in actin. The limiting anisotropy of DNS attached to Tyr-69 was 0.280 (Miki & dos Remedios, 1990), while the fundamental anisotropy of the DNS-moiety was reported to be 0.352 (Kasprzak et al., 1988). From these data, the minimum and maximum values of κ^2 were determined according to the method of Dale et al. (1979). For an average distance of 2.79 nm in the case of G-actin, an upper limit of 1.6 nm in the distribution width could be due to orientation.

DNS-Cl was conjugated to the amino group joined to the C-3 atom (Cϵ) of the phenol ring of Tyr-69. There are five single bonds and one phenol ring between the α-carbon of Tyr-69 and the DNS fluorophore. For a linker arm of this length, several angstroms in FWHM could be accounted for by its flexibility, although the exact contribution of this factor is difficult to estimate. According to the atomic structure of actin, the distances between the Cα or the Cϵ of Tyr-69 and the N^6 of adenine are 2.2 and 1.9 nm (Cϵ_1) or 1.7 nm (Cϵ_2), respectively. The distance determined from fluorescence resonance energy transfer is significantly longer than the above values, but this difference can be explained when the linker arm of fluorophore is taken into consideration. The possibility may not be excluded that the introduction of the fluorophore distorts the native structure of actin. But this distortion may not be significant because the labeled actin retains its activity; i.e., it interacts with DNase I and it polymerizes upon addition of salts in the presence of phalloidin (Miki, 1991).

The contributions of the orientation factor and the linker arm flexibility are not enough to explain the large FWHM in the present analysis. A broad distance distribution has also been observed in fluorescence resonance energy transfer measurements of 3-phosphoglycerate kinase which consists of two globular domains. Haran et al. (1992) showed a wide distribution of distances (FWHM $\leq 3.1 \pm 0.2$ nm) between probes attached to two globular domains of the protein. On the other hand, the crystallographic analysis of D-maltodextrin binding protein (MBP) has revealed two stable forms: (1) the two domains become closer and the cleft between two domains is relatively narrowed (the closed form), and (2) the two domains are farther apart and the cleft is wide open (the open form). The open and closed forms are interconverted by bending around a hinge between the two domains. The overall motion in this protein is such that residues at opposite ends of the face have moved by up to 2.0 nm (Sharff et al., 1992). It is further proposed that the open and closed forms exist in an equilibrium, where ligand binding stabilizes the closed form. In solution, actin may take several stable forms and exist in a dynamic equilibrium between these states in a physiological time scale. Several physical methods that measure rotational relaxation indicate motions in actin in the time region from nanoseconds to milliseconds. Fluorescence

anisotropy decay measurements of εATP/ADP bound to actin showed no segmental mobility of this site in the nanosecond time scale, but measurements of transient absorption and phosphorescence anisotropy (Yosimura et al., 1984) or saturation transfer electron paramagnetic resonance spectra (Thomas et al., 1979) indicate internal motions within the actin molecule in the microseconds to millisecond time region. Although a conformational change from one substate to another is slow on the nanosecond time scale, flexibility on a long time scale can lead to heterogeneity in conformation and consequently distance distributions as determined on the nanosecond time scale. The distance distribution from fluorescence resonance energy transfer may be regarded as the instantaneous static picture of the actin molecule in solution. It should be noted here that the binding of tropomyosin/troponin or S1 induces a significant immobilization of internal motions within F-actin in the microsecond to millisecond time region (Thomas et al., 1979; Mihashi et al., 1983; Yoshimura et al., 1984). This immobilization reduces the extent of heterogeneity in the actin structure and consequently results in decrease of FWHM in accordance with the present results (Table 2). Further study of the resonance energy transfer measurements is necessary for better understanding about the dynamic structure of actin in solution.

ACKNOWLEDGMENT

We thank Dr. H. Suda at Tokai University and Dr. K. Kinosita at Keio University for their useful suggestions.

REFERENCES

Bennett, W. S., & Huber, R. (1984) *CRC Crit. Rev. Biochem. 15*, 291–384.
Botts, J., Takashi, R., Torgerson, P., Hozumi, T., Muhlrad, A., Mornet, D., & Morales, M. F. (1984) *Proc. Natl. Acad. Sci. U.S.A. 81*, 2060–2064.
Chantler, P. D., & Gratzer, W. B. (1975) *Eur. J. Biochem. 60*, 67–72.
Cummins, P., & Perry, S. V. (1973) *Biochem. J. 133*, 765–777.
Dale, R. E., Eisinger, J., & Blumberg, W. E. (1979) *Biophys. J. 26*, 161–194.
dos Remedios, C. G., Miki, M., & Barden, J. A. (1987) *J. Muscle Res. Cell Motil. 8*, 97–117.
Eis, P. S., & Lakowicz, J. R. (1993) *Biochemistry 32*, 7981–7993.
Engel, J., Fasold, H., Hulla, F. E., Waechter, F., & Wegner, A. (1977) *Mol. Cell. Biochem. 18*, 3–13.
Fairclough, R. H., & Cantor, C. R. (1978) *Methods Enzymol. 48*, 347–379.
Förster, T. (1948) *Ann. Physik. 2*, 55–75.
Haas, E., Wilchek, M., Katchalski-Katzir, E., & Steinberg, I. Z. (1975) *Proc. Natl. Acad. Sci. U.S.A. 72*, 1807–1811.
Haran, G., Haas, E., Szpikowska, B. K., & Mas, M. T. (1992) *Proc. Natl. Acad. Sci. U.S.A. 89*, 11764–11768.
Holland, D. R., Tronrud, D. E., Pley, H. W., Flaherty, K. M., Stark, W., Jansonius, J. N., McKay, D. B., & Matthew, B. W. (1992) *Biochemistry 31*, 11310–11316.
Holmes, K. C., Popp, D., Gebhard, W., & Kabsch, W. (1990) *Nature (London) 347*, 44–49.
Ishiwata, S., & Fujime, S. (1972) *J. Mol. Biol. 68*, 511–522.
James, E., Wu, P. G., Stites, W., & Brand, L. (1992) *Biochemistry 31*, 10217–10225.
Kabsch, W., Mannherz, H. G., Suck, D., Pai, E. F., & Holmes, K. C. (1990) *Nature (London) 347*, 37–44.
Kasprzak, A. A., Takashi, R., & Morales, M. F. (1988) *Biochemistry 27*, 4512–4522.
Kenner, R. A., & Neurath, H. (1971) *Biochemistry 10*, 551–557.
Kinosita, K., Kawato, S., & Ikegami, A. (1977) *Biophys. J. 20*, 289–305.
Kouyama, T., Kinosita, K., & Ikegami, A. (1985) *Biophys. J. 47*, 43–54.
Kouyama, T., Kinosita, K., & Ikegami, A. (1989) *Eur. J. Biochem. 182*, 517–521.
Lakowicz, J. R. (1983) *Principles of Fluorescence Spectroscopy*, Plenum Press, New York.
Lehrer, S. S., & Kerwar, G. (1972) *Biochemistry 11*, 1211–1217.
Liang, P. (1941) *Org. Synth. 21*, 105–107.
Lorenz, M., Popp, D., & Holmes, K. C. (1993) *J. Mol. Biol. 234*, 826–836.
Mannherz, H. G., Goody, R. S., Konrad, M., & Nowak, E. (1980) *Eur. J. Biochem. 104*, 367–379.
Mihashi, K., & Wahl, Ph. (1975) *FEBS Lett. 52*, 8–12.
Mihashi, K., Yoshimura, H., Nishio, T., Ikegami, A., & Kinoshita, K. (1983) *J. Biochem. (Tokyo) 93*, 1705–1707.
Miki, M. (1990) *Eur. J. Biochem. 187*, 155–162.
Miki, M. (1991) *Biochemistry 30*, 10878–10884.
Miki, M., & Wahl, Ph. (1984) *Biochim. Biophys. Acta 786*, 188–196.
Miki, M., & dos Remedios, C. G. (1990) *Biochem. Int. 22*, 125–132.
Miki, M., & Iio, T. (1993) *J. Biol. Chem. 268*, 7101–7106.
Miki, M., Barden, J. A., dos Remedios, C. G., Phillips, L., & Hambly, B. D. (1987) *Eur. J. Biochem. 165*, 125–130.
Miki, M., O'Donoghue, S. I., & dos Remedios, C. G. (1992) *J. Muscle Res. Cell Motil. 13*, 132–145.
Neidl, C., & Engel, J. (1979) *Eur. J. Biochem. 101*, 163–169.
Oosawa, F. (1983) in *Muscle and Nonmuscle Motility* (Stracher, A., Ed.) Vol. 1, pp 151–216, Academic Press, New York.
Ringe, D., & Petsko, G. A. (1985) *Prog. Biophys. Mol. Biol. 199*, 525–537.
Secrist, A. J., Barrio, J. R., Leonard, N. J., & Weber, G. (1972) *Biochemistry 11*, 3499–3506.
Sharff, A. J., Rodseth, L. E., Spurlino, J. C., & Quiocho, F. A. (1992) *Biochemistry 31*, 10657–10663.
Small, E. W., & Isenberg, I. (1976) *Biopolymers 15*, 1093–1100.
Stryer, L. (1978) *Annu. Rev. Biochem. 47*, 819–846.
Stryer, L., & Haugland, R. P. (1967) *Proc. Natl. Acad. Sci. U.S.A. 58*, 719–726.
Tirion, M. M., & ben-Avraham, D. (1993) *J. Mol. Biol. 230*, 186–195.
Thomas, D. D., Seidel, J. C., & Gergely, J. (1979) *J. Mol. Biol. 132*, 257–2643.
Weeds, A. G., & Pope, B. (1977) *J. Mol. Biol. 111*, 129–157.
Yoshimura, H., Nishio, T., Mihashi, K., Kinosita, K., & Ikegami, A. (1984) *J. Mol. Biol. 179*, 453–467.